



HAL
open science

Contemporary image-based methods for measuring passive mechanical properties of skeletal muscles in vivo

Lynne Bilston, Bart Bolsterlee, Antoine Nordez, Shantanu Sinha

► To cite this version:

Lynne Bilston, Bart Bolsterlee, Antoine Nordez, Shantanu Sinha. Contemporary image-based methods for measuring passive mechanical properties of skeletal muscles in vivo. *Journal of Applied Physiology*, 2019, 126 (5), pp.1454-1464. 10.1152/jappphysiol.00672.2018 . hal-03333540

HAL Id: hal-03333540



<https://hal.science/hal-03333540>

Submitted on 20 Apr 2023

HAL is a multi-disciplinary open access archive for the deposit and dissemination of scientific research documents, whether they are published or not. The documents may come from teaching and research institutions in France or abroad, or from public or private research centers.

L'archive ouverte pluridisciplinaire **HAL**, est destinée au dépôt et à la diffusion de documents scientifiques de niveau recherche, publiés ou non, émanant des établissements d'enseignement et de recherche français ou étrangers, des laboratoires publics ou privés.

Contemporary image-based methods for measuring passive mechanical properties of skeletal muscles in vivo

 Lynne E. Bilston,^{1,2}  Bart Bolsterlee,^{1,3*} Antoine Nordez,^{4,5*} and Shantanu Sinha^{6*}

¹Neuroscience Research Australia, Randwick, New South Wales, Australia; ²Prince of Wales Clinical School, University of New South Wales, Randwick, New South Wales, Australia; ³Graduate School of Biomedical Engineering, University of New South Wales, Kensington, New South Wales, Australia; ⁴Health and Rehabilitation Research Institute, Auckland University of Technology, Auckland, New Zealand; ⁵Movement, Interactions, Performance Laboratory (EA 4334), Faculty of Sport Sciences, University of Nantes, Nantes, France; and ⁶Muscle Imaging and Modeling Laboratory, Department of Radiology, University of California, San Diego, California

Submitted 1 August 2018; accepted in final form 13 September 2018

Bilston LE, Bolsterlee B, Nordez A, Sinha S. Contemporary image-based methods for measuring passive mechanical properties of skeletal muscles in vivo. *J Appl Physiol* 126: 1454–1464, 2019. First published September 20, 2018; doi:10.1152/jappphysiol.00672.2018.—Skeletal muscles' primary function in the body is mechanical: to move and stabilize the skeleton. As such, their mechanical behavior is a key aspect of their physiology. Recent developments in medical imaging technology have enabled quantitative studies of passive muscle mechanics, ranging from measurements of intrinsic muscle mechanical properties, such as elasticity and viscosity, to three-dimensional muscle architecture and dynamic muscle deformation and kinematics. In this review we summarize the principles and applications of contemporary imaging methods that have been used to study the passive mechanical behavior of skeletal muscles. Elastography measurements can provide in vivo maps of passive muscle mechanical parameters, and both MRI and ultrasound methods are available (magnetic resonance elastography and ultrasound shear wave elastography, respectively). Both have been shown to differentiate between healthy muscle and muscles affected by a broad range of clinical conditions. Detailed muscle architecture can now be depicted using diffusion tensor imaging, which not only is particularly useful for computational modeling of muscle but also has potential in assessing architectural changes in muscle disorders. More dynamic information about muscle mechanics can be obtained using a range of dynamic MRI methods, which characterize the detailed internal muscle deformations during motion. There are several MRI techniques available (e.g., phase-contrast MRI, displacement-encoded MRI, and “tagged” MRI), each of which can be collected in synchrony with muscle motion and postprocessed to quantify muscle deformation. Together, these modern imaging techniques can characterize muscle motion, deformation, mechanical properties, and architecture, providing complementary insights into skeletal muscle function.

biomechanics; diffusing tensor imaging; elastography; magnetic resonance imaging; ultrasound

INTRODUCTION

As the primary actuator in the human body, research aimed at understanding the mechanical behavior of skeletal muscles has been performed for more than a century (e.g., 14). From this wealth of research, it is now clear that even when passive, skeletal muscles have very complex mechanical behavior and are anisotropic, nonlinearly viscoelastic tissues (e.g., 34, 87,

88). Skeletal muscle's anisotropy (different mechanical behavior in different directions) arises from its anisotropic microstructure, with the parallel myofibers arranged into fascicles. Nonlinear viscoelastic behavior in skeletal muscle can be observed from an increasing apparent “stiffness” as muscles are stretched (i.e., nonlinear elasticity) and reduction in the force in a stretched passive muscle over time (i.e., viscoelastic relaxation). This behavior is thought to arise from similar sources as in other soft tissues, namely, the inherent nonlinear viscoelasticity of constituents, interactions between these constituents, and progressive recruitment of these constituents under load.

* B. Bolsterlee, A. Nordez, and S. Sinha contributed equally to this work.
Address for reprint requests and other correspondence: L. E. Bilston, Neuroscience Research Australia, Barker St., Randwick, NSW 2031, Australia (e-mail: L.Bilston@neura.edu.au).

Although the focus of this mini-review is the passive properties of skeletal muscle, contractions alter the mechanical properties of muscle. Active muscle properties are beyond the scope of this review. However, muscle contractions can also alter the subsequent passive properties in some circumstances. For example, a muscle contraction can induce a small amount of thixotropy postcontraction, where a muscle appears stiffer until an apparent “yield stress” is overcome (71) during subsequent passive elongation of the muscle.

In the last 30 years, researchers’ attention has turned to methods to make measurements of muscle mechanics *in vivo*, as these are thought to better represent “real-world” conditions, and recently, imaging technology has begun to enable *in vivo* measurements. However, the complex mechanical behavior of muscles gives rise to several practical and methodological challenges for research in human muscle mechanics, particularly for the image-based methods that we focus on here. Many of these are discussed in more detail throughout this review, but they include the need to carefully control the deformation or loading state of a muscle and ensuring that a muscle is truly passive during measurements, as both make substantial differences in the mechanical parameters obtained.

This review outlines four key image-based methods that have been used to quantify skeletal muscle mechanics and aims to provide critical evaluation of their strengths and weaknesses and applications in both healthy subjects and patient groups. The first of these is magnetic resonance elastography (MRE), which relies on transmission of an external vibration to the muscle, using MRI to measure the resulting propagation of displacement waves in the tissue. Maps of shear modulus are then calculated. The second, ultrasound shear wave elastography (SWE), is based on similar principles but uses ultrasound rather than MRI. Both these methods rely on the physics of wave propagation through elastic or viscoelastic media, where wave speed is related to the mechanical properties of the material, with waves traveling faster through stiffer material. In strain-based ultrasound elastography, the effect of the sonographer compressing the tissue with the transducer is used to create qualitative stiffness maps, relying on the principle that stiffer tissue regions will deform less than softer regions. We focus here on quantitative methods and will not further discuss strain elastography. Third, diffusion tensor imaging (DTI) gives insight into the microstructure of the muscle, by quantifying the diffusion of water molecules within the tissue, and relies on this being different along the direction of muscle fascicles from perpendicular to it. Most of these methods provide quasi-static measurements of mechanical behavior as they require seconds to minutes to acquire, although some ultrasound SWE implementations can provide more rapid measurements. The fourth approach, dynamic imaging, aims to characterize the deformation of muscle during motion and can be either ultrasound- or MRI-based. Finally, imaging is often combined with other biomechanical measurements, such as the combination of ultrasound with dynamometry to measure muscle deformation to match with joint torques (e.g., 42), to give a picture of the mechanical behavior of muscle. These latter methods typically do not yield the intrinsic mechanical properties (e.g., shear modulus) of muscle and their variation across a muscle but do provide whole muscle length-tension or fascicle-tension curves.

MAGNETIC RESONANCE ELASTOGRAPHY OF SKELETAL MUSCLE

Methods. MRE of skeletal muscle involves applying an external sinusoidal vibration at a given frequency that is synchronized to a displacement-sensitive MRI acquisition to the muscle. By varying the temporal offsets between the mechanical vibration and the imaging acquisition, the displacement of each pixel in the image domain throughout a vibration cycle is obtained. These data are then postprocessed to calculate the shear modulus at each point in the tissue of interest, a measure of the resistance of the tissue to shear deformation. This postprocessing typically involves filtering the data and then applying an inversion algorithm that either solves the linear viscoelastic wave equation or solves a simplified version thereof. A more detailed review of the technical details of MRE in muscle is given by Bilston and Tan (8). Figure 1 shows a typical MRE setup, displacement wave data at 60 Hz, and a calculated shear modulus elastogram from a healthy adult male volunteer.

The majority of MRE studies of muscle properties assume that muscle is isotropic (e.g., 25, 39, 48, 75, 85), and thus the reported values represent an “average” in all directions and may not be as sensitive to physiologically relevant differences in muscle mechanical properties, such as those that may affect the muscle fiber direction more than the cross-fiber direction (e.g., 15). More recently, anisotropic MRE methods have been developed (e.g., 74) that consider muscle to be a transversely isotropic material. These methods have been used to study both healthy and damaged or disease-affected muscle (e.g., 38, 73) as discussed below. To extract anisotropic muscle properties, the most robust methods require knowledge of the muscle fascicle directions, which can be obtained from diffusion imaging (see the section devoted to this technique below). These directions, together with the displacement data, can be used to estimate the anisotropic elastic component of the shear modulus both along the muscle fascicle direction and perpendicular to it, as well as to provide an estimate of the viscous behavior (e.g., 74).

Although MRE can be used to measure both the elastic and the viscous properties of muscle and other tissues, many early studies reported only the elastic properties (e.g., 4, 6, 13, 18, 41). Multifrequency MRE performs measurements using multiple vibration frequencies, which can give insight into the strain rate-sensitive viscoelastic behavior of muscle to assess the viscous nature of the tissue (e.g., 19).

All the above methods provide only the linear viscoelastic properties, i.e., those at very small deformations. Physiologically, we are typically interested in the nonlinear behavior over the full range of physiological deformations that a muscle undergoes. There is one recent study that has attempted to measure the nonlinear behavior of skeletal muscle, by conducting MRE at a range of quasi-static stretch levels (84). Another recent study has observed increased shear moduli when muscle is indented to induce damage (68). Further work is required to embed such experimental approaches in a robust theoretical framework that considers both muscle anisotropy and the complexity of the nonlinear mechanics of muscle.

Critical evaluation. The major strength of MRE is its capacity to provide three-dimensional (3-D) “maps” of muscle viscoelastic properties *in vivo*, including variation in properties

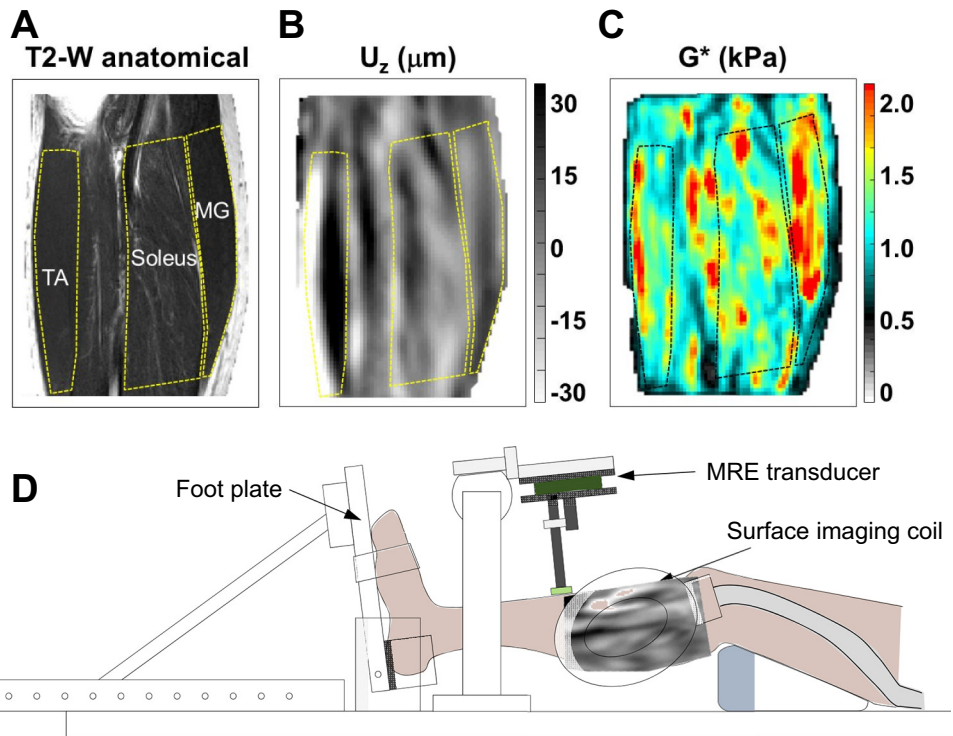


Fig. 1. Typical data set and magnetic resonance elastography (MRE) setup for measuring calf muscle mechanical properties. *A*: T2-weighted (T2-W) anatomical image indicating the tibialis anterior (TA), soleus, and medial gastrocnemius (MG) muscles from an oblique slice through the lower leg. *B*: sample displacement wave image for displacements in the through-plane direction (U_z). *C*: calculated isotropic shear modulus map. G^* is the magnitude of the linear viscoelastic shear modulus. *D*: MRE setup used to obtain the above data set. [Courtesy of A. Hatt and L. E. Bilston.]

between muscles and within a muscle. With further development to reduce the impact of some of the present limitations, it has the potential to provide useful physiological and clinical information in skeletal muscle applications.

Many of the limitations of MRE are not specific to its application to muscle. These include a lack of standardization of either the imaging or the analysis methods, with different transducer types, vibration frequencies, and MRI sequences used. Analysis methods also remain a critical challenge for the field, as the calculation of the shear modulus from the image data is a numerically ill-conditioned problem and is sensitive to both noise in the images and low displacement wave amplitude (due to attenuation of the propagating vibration). Also arising from the numerical methods used is a limited spatial resolution, since at least two, and often four, adjacent pixels are used to calculate the shear moduli in any given pixel. These issues also apply to anisotropic MRE, and development of robust analysis methods for anisotropic tissues is still an open challenge.

Anisotropic MRE has been partially validated in muscle, via comparison of anisotropy measures against both phantoms and *ex vivo* muscle tissue (74), although quantitative comparisons of the anisotropic shear moduli and viscous components are few and far between, in part because of the differences in loading rate achievable with rheometers and MRE. As result of this wide variation in methods and the use of relatively small samples in many studies, reported results can differ between research laboratories. Another key concern is that due to the nonlinear mechanical behavior of muscle, the loading state of the muscle can strongly affect the measured properties (68, 84). To compare results, it therefore is important to standardize the muscle passive tension, perhaps by ensuring that the muscle is completely slack, and also to ensure that the transducer does not load the muscle.

There is a very limited quantity of data that suggest that the vibration needed for MRE does not invoke muscle activity in the tongue (15, 20), and some studies show that mild muscle contraction increases the measured shear moduli in MRE experiments (e.g., 41, 48), suggesting that MRE may be sensitive to contraction-induced stiffness changes. The latter not only could mean that MRE could be useful for measuring stiffness changes due to low-level contractions but also means that if a muscle is not completely passive during an MRE measurement, this could introduce bias in the reported stiffness. Finally, MRE measurements take a few minutes to perform. It is thus not practical for dynamic studies and is challenging to use for muscle contraction studies, as only low-level contractions can be held constant for the duration of the acquisition, or repeated contractions must be used and data acquisition “gated” to the contractions. For anisotropic MRE, which also requires diffusion measurements to identify the muscle fiber directions, this adds another few minutes to each acquisition, further constraining its use to static measurements.

Applications. MRE has demonstrated potential for measuring mechanical properties *in vivo*, and results to date suggest that it has potential to be a useful clinical tool for tracking muscle degeneration (73), injury (39, 43), and the effects of hormonal and other disorders on muscles (e.g., 13, 15, 63, 66). MRE has been applied in mostly small studies of clinical populations and in animal models of disease. One study showed that changes in the stiffness of the muscles of men with hypogonadism could be detected using MRE (13). A small study of patients with hyperthyroidism showed lower stiffness before treatment, with muscle properties returning to control values after treatment (5). Green et al. (39) showed that muscle stiffness followed the same time course as pain symptoms after eccentric muscle damage. Brown et al. (15) studied patients

with obstructive sleep apnea, reporting lower tongue stiffness in the direction of the genioglossus muscle fibers than in matched healthy controls, consistent with greater upper airway collapsibility in patients. In a mouse model of muscular dystrophy, Qin et al. (73) found that the mechanical anisotropy was a sensitive marker of muscle necrosis, detecting changes earlier than diffusion imaging. McCullough et al. used MRE in patients with myositis, finding that relaxed thigh muscles of patients have significantly lower shear modulus than those of controls (63). See also Kim et al. (50) for a review of pediatric applications.

ULTRASOUND SHEAR WAVE ELASTOGRAPHY

Methods. As for MRE, ultrasound SWE consists of applying a mechanical perturbation to induce the propagation of a shear wave. The different ultrasound SWE techniques have been described previously in detail (e.g., 35, 78), and some are available in commercial ultrasound scanners (e.g., SuperSonic Imagine, Siemens, and Toshiba). Briefly, the mechanical perturbation can be applied using an external mechanical actuator or remotely with ultrasound. Ultrasound is then used to track the shear wave propagation. Since ultrasound can provide a high temporal resolution (frame rate up to 20 kHz), it is possible to induce the shear wave propagation with a transient excitation (7). A transient excitation would provide an easier tracking of the shear wave because boundary conditions are less problematic (35). In addition, a transient excitation enables us to analyze the shear wave propagation as a function of the frequency [i.e., shear wave spectroscopy (36)]. Shear wave spectroscopy can

be used to account for the viscosity (36) and the guided wave propagation that occurs in stiff and thin tissues (16).

Critical evaluation. A previous study showed a good correlation ($R^2 = 0.94$) between the Young’s modulus measured using a material-testing machine during passive stretching of an animal muscle and the shear modulus measured using ultrasound SWE (27). It validated the shear modulus measurement as a relevant outcome for measuring muscle mechanical properties. In addition, several studies showed that this technique is reliable at rest (e.g., 54) and during passive muscle stretching (e.g., 58; Fig. 2). Compared with MRE, this technique is relatively low cost and relatively easy to access. Although spatial resolution (i.e., pixel size) in ultrasound SWE can be slightly better than for MRE, both require averaging over many pixels for reliable results. In addition, the measurement can be performed in <100 ms (7). Thus, the temporal resolution, which can reach up to 1–4 Hz, can enable tracking of the changes in muscle mechanical behavior during contractions and/or passive stretching to analyze the nonlinear behavior of muscle. It is also easy to use in a biomechanics laboratory and to synchronize with other measurements (e.g., force and/or motion).

As with all ultrasound measurements, ultrasound SWE requires appropriate practice to account for probe location, orientation, and pressure. The practice is completed when the experimenter is able to perform reliable measurements (intra-day or between days depending on the experimental design). In addition, it measures the shear wave velocity in 2-D, providing an incomplete picture of the muscle mechanical behavior. Anisotropy can be easily measured in fusiform muscles be-

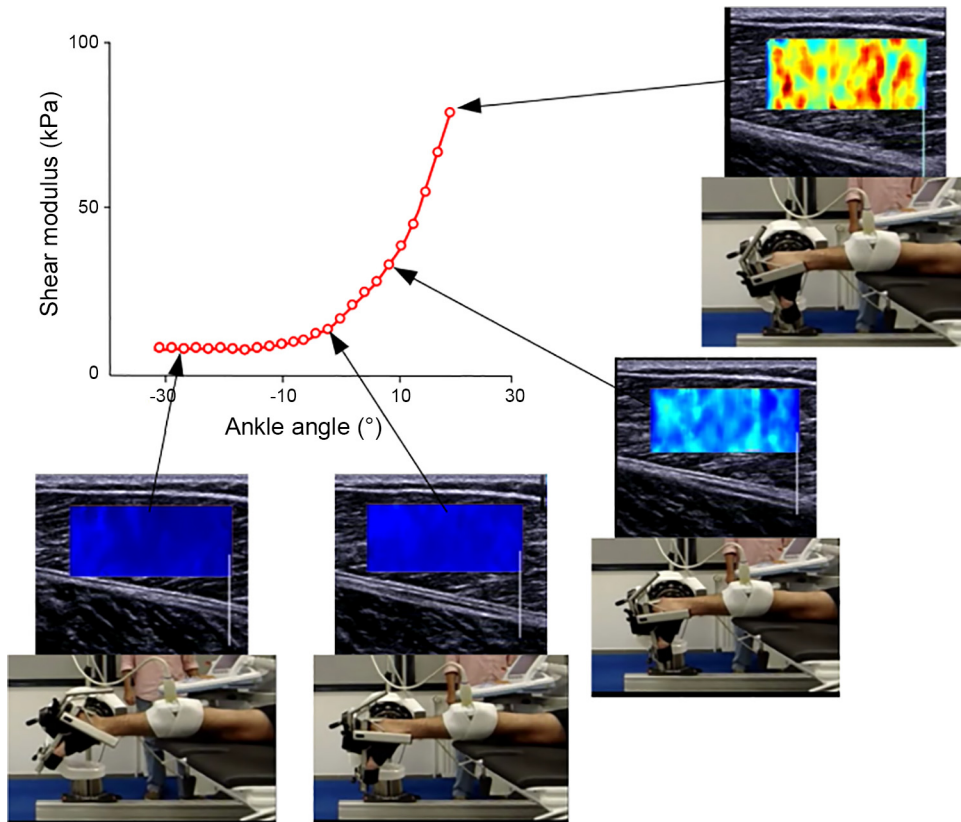


Fig. 2. Typical example of changes in shear modulus of the gastrocnemius medialis during passive dorsiflexion performed at 2°/s. Le Sant et al. (57) replicated this measurement on 13 locations among all the plantar flexor muscles. [Adapted from Maisetti et al. (58).]

cause in that case the shear wave propagation can be analyzed with respect to the direction of muscle fibers (36). Because it is impossible to measure the shear wave velocity along the muscle fiber direction of pennate muscles (i.e., the large majority of human muscles), anisotropy is more problematic here than for fusiform muscles. In the case of a pennate muscle, we recommend performing the measurement along the shortening-lengthening axis of the muscle (27). Thus, the measurement reflects the muscle behavior that actually influences the motion of the joint, exactly as can be done in an isolated muscle using a material-testing machine (27).

A recent study shows the feasibility of performing 3-D measurements in the muscle using matrix probes (37). In the future, this innovative technique will provide a better understanding of 3-D muscle behavior during stretching and contractions. In addition, measurements of muscle viscosity would provide a deeper understanding of muscle behavior and could become a new relevant clinical outcome in several diseases.

Applications. In the last couple of years, there has been an explosion of publications using SWE to quantify human muscle behavior, possibly thanks to commercialized devices that are accessible in many fields of research (biomechanics, sport sciences, physiotherapy, and medicine). Thus, the applications are very numerous and cannot be exhaustively reviewed here. The first field of application is the evaluation of muscle in diseases that increase muscle stiffness such as Duchenne muscular dystrophy (53) or contractures induced by stroke (26, 56). Interestingly, Le Sant et al. (57) have shown that it is possible to map the shear modulus of plantar flexors during a passive dorsiflexion and thus provide a better understanding of their contributions to the passive stiffness at the joint level. This protocol could be relevant for the evaluation of contracture in a muscle group. Second, Hug et al. (46) showed that changes in muscle shear modulus are linearly related to the changes in both passive and active muscle force. This result was used to measure the muscle and tendon slack length (45), to analyze the acute effects of stretching (67), warm-up (65), massage (29), or eccentric exercise that induces muscle damage (55).

DYNAMIC MRI METHODS

Methods. The objective quantification of regional muscle deformation is a valuable clinical tool to evaluate normal and diseased muscle. MRI has been used, in muscle tissue, to quantify either displacement or velocity in a single 2-D slice, with some of the earliest development of the cine phase-contrast technique reported by Asakawa et al. (3), with the quantification of the motion of the rectus femoris after tendon transfer surgery (2), and subsequently extended to multislice or 3-D volumes (49, 59, 61, 92). Strain and strain rate are kinematic properties that can be derived from the displacement (strain)- and velocity (strain and strain rate)-encoded magnetic resonance (MR) images and have been used to characterize myocardial, lingual, and skeletal deformation (30, 31, 52, 77). Strain describes how the tissue is deformed with respect to a reference state and requires tissue tracking. Strain rate describes the rate of regional deformation and does not require tracking or a reference state since it is an instantaneous measure. A positive strain or strain rate indicates a local expansion whereas a negative strain or strain rate indicates a local contraction.

Dynamic imaging sequences. There are three motion-encoding sequences commonly used to monitor skeletal muscle dynamics: velocity-encoded phase-contrast (VE-PC; 59), displacement encoding with stimulated echoes (DENSE; 49), and MR tagging, where the tagged lines/grid are tracked to quantify strain (28). In addition,

harmonic phase (HARP) analysis of spin-tagged lines and direct strain-encoded cardiac magnetic resonance (SENC) have been applied to quantify cardiac motion (52, 91). The sequences are acquired gated to the muscle motion to study muscle tissue deformation during passive and active muscle activation (28, 59, 92). In VE-PC MRI, flow-encoding gradients are incorporated into a gradient echo to encode the velocity in the phase; a three-directional velocity-encoding sequence is used to monitor the velocity vector. DENSE MRI directly encodes the displacement as the phase of a voxel but, since it is a stimulated echo acquisition, suffers from a loss in signal-to-noise ratio by a factor of 2 compared with the VE-PC method. However, DENSE MRI is useful for encoding displacements over long time intervals compared with T1 relaxation times. MR tagging techniques allow lines or grids to be superposed on the anatomical image; these lines and grids are created by specially designed radio frequency pulses to saturate the protons with the desired pattern [spatial modulation of magnetization (SPAMM)]. The tracking of the tag lines is used to quantify muscle deformation. However, manual or semiautomated tracking is usually tedious and time-consuming. Further limitations of this technique are that tag lines fade because of T1 effects, spacing of the tag lines/grids is much bigger than the voxel resolution, and tagging is usually done in 2-D rather than in 3-D.

Dynamic MRI hardware. Several groups have developed MR-compatible hardware to execute repeated passive or active motion (28, 49, 59, 61, 92). One such foot pedal design has been used in several studies that cover the dynamics of calf muscle under passive plantar flexion and active isometric flexion, plantar flexion, and dorsiflexion to evaluate normal, atrophied, and aging muscle (21, 59, 81, 82). In this design, the foot rests on a carbon fiber plate with an embedded optical force transducer. For passive plantar flexion, the pedal is attached to a piston-cylinder device, controlled by computer-driven servomotor and connected by tubing to the piston-cylinder. The angular motion of the foot pedal is monitored by the digital output from the computer, which also generates an R wave-like trigger pulse used to gate the acquisition.

Analysis. The calculation of strain or strain rate tensor is similar, with the former using the displacement vector and the latter using the velocity vector (32, 81). In brief, for VE-PC data, phase images are corrected for phase shading artifacts and denoised with an anisotropic diffusion filter. The 2-D spatial gradient of the velocity vector, L , is calculated from the spatial gradient of the velocity components v_x and v_y . The symmetric part of the strain rate tensor is calculated from $D = 0.5(L + L^T)$ (where L^T is the transpose of L) and diagonalized. The negative eigenvalue during passive plantar flexion is denoted as SR_{fiber} (where SR is strain rate) since its eigenvector is closest to the muscle fiber direction and, in the dorsiflexion stage, the negative eigenvalue changes to the orthogonal direction (Fig. 3). The maximum shear strain is determined by rotating the 2-D strain rate tensor in the principal basis by 45° .

Critical evaluation. Dynamic imaging is not a real-time technique and relies on the repeatability of the motion. This limits acquisition to single 2-D slice imaging. The clinical application of 3-D strain tensors awaits the development of fast 3-D, three-directional encoded sequences; a recent compressed-sensing 3-D, three-directionally encoded VE-PC approach that allows acquisition in ~ 2 min shows promise (61).

Applications. Huijing et al. showed, in cadavers using such MRI techniques, the presence of local strains within calf muscles even when global strain was not evident (47). Yaman et al. demonstrated, using high-resolution 3-D MRI and calculations of large deformations using nonrigid transformations, significant heterogeneous local strains in all muscles of the lower leg concomitant to global length changes in the gastrocnemius muscle-tendon complex (90). Strain rate tensor imaging of the lower leg was used to study age-related differences between younger and older subjects. Under passive plantar flexion, no significant differences with age were seen in strain indexes in the medial gastrocnemius; however, regional differences were

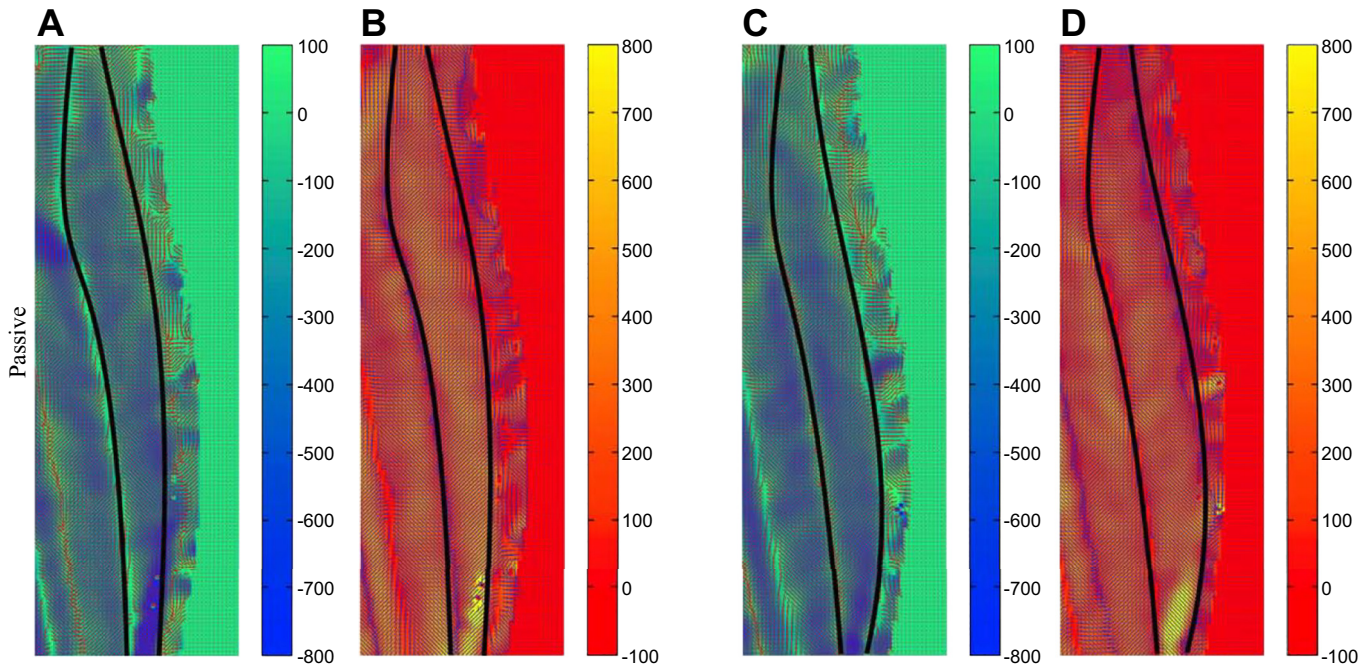


Fig. 3. Eigenvectors (lines) corresponding to the eigenvalues of the strain rate (SR) tensor are shown superposed on the eigenvalue images for a young subject (81). A zoomed area of the medial gastrocnemius is shown during passive joint rotation (left \rightarrow right): $SR_{in-plane}$, negative eigenvalue, dorsiflexion (A); SR_{fiber} , positive eigenvalue, dorsiflexion (B); SR_{fiber} , negative eigenvalue, plantar flexion (C); and $SR_{in-plane}$, positive eigenvalue, plantar flexion (D). The pixel color is assigned according to the magnitude of the eigenvalue and ranges from 0 (green) to -800 s^{-1} (blue) for the negative eigenvalue images and from 0 (red) to 800 s^{-1} (yellow) for the positive eigenvalue images (note that values were scaled by 1,000). In dorsiflexion, the negative strain rate direction is approximately perpendicular (A), and the positive strain rate is approximately parallel to the fiber direction (B), whereas the reverse is true for the plantar flexion phase (C and D). $SR_{in-plane}$ is the strain of the fiber cross section in the plane of the image (the 3rd component in the slice direction is not calculated here as only 1 slice is acquired). [Borrowed with permission from Sinha et al. (81).]

found (81). Maximum shear strain was shown to correlate with force in the same cohort of young and old subjects (82). Strain rate tensor imaging of disuse atrophy also identified maximum shear strain as a significant predictor of force loss with disuse (59). The authors speculate that the dependence of force on shear strain may be related to the mechanical properties of the extracellular matrix that may get stiffer with age (59, 82).

Recently, the feasibility of volumetric strain mapping in the calf muscles during passive plantar flexion using multislice VE-PC imaging was demonstrated, which may have application as a surrogate measure of intramuscular pressure (49). DENSE imaging was used to explore the effect of activation and morphology on strain patterns in the hamstring muscles, and this study showed that localized elevated strains and a narrow proximal aponeurosis may be risk factors for hamstring injury (32).

DIFFUSION IMAGING

Methods. DTI is an MRI technique that provides a measurement of the extent and direction of diffusion of water molecules. DTI has long been used to reconstruct the neuroanatomy of the brain. Its application to muscle fibers is rendered more difficult because of the much shorter T2 relaxation times with consequent decrease in signal-to-noise ratio compared with the brain. However, recently, DTI has been applied successfully to characterize muscle structure in terms of various DTI parameters, such as its fractional anisotropy (a longitudinal-to-cross-sectional ratio of diffusion within the fiber), primary, secondary, and tertiary eigenvectors. The diffusion properties allow the measurement of 3-D lengths and orientations of muscle fibers in skeletal muscles and, potentially, the fiber length-to-

fiber cross section ratio and ellipticity of the cross section. The fiber orientation measurements are based on the principle that diffusion of water molecules occurs primarily in the axial direction of muscle fibers because radial direction diffusion is obstructed by (presumably) cell membranes and intracellular obstructions (51). Previous studies have shown that DTI measurements of the primary direction of diffusion are aligned with the long axis of muscle fascicles (23, 76). The theoretical basis of DTI and the details of the data acquisition and postprocessing procedures are beyond the scope of this review but can be found in two recent review articles (24, 69).

DTI-based measurements of fiber orientations can be made at a great number of locations in a muscle and so provide useful information for characterizing the anisotropic mechanical behavior of muscle tissue (73, 74). The 3-D fiber orientations can also be used to generate curves that follow the fiber orientation throughout a muscle. This procedure is called DTI tractography, and the curves are called fiber tracts. Fiber tracts are not direct representations of muscle fibers or muscle fascicles (which are bundles of muscle fibers), as the number of fiber tracts generated within a muscle can be arbitrarily chosen and the curves are infinitely thin (i.e., 1-D). However, fiber tracts follow the direction of fibers throughout a muscle, so their lengths and orientations reflect the fascicle lengths (defined as the length of a bundle of fibers from its origin to insertion on tendons or aponeuroses) and pennation angles of the muscle. Tractography has been used successfully to measure the 3-D architecture of various human muscles in vivo [e.g., 9, 33, 93; see Fig. 4, which shows examples of muscle fibers

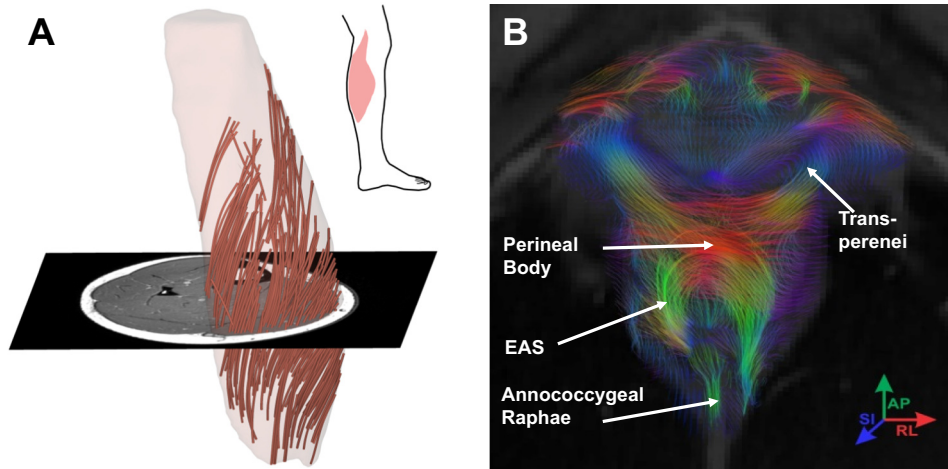


Fig. 4. Examples of three-dimensional reconstruction of the architecture of the human medial gastrocnemius muscle (A) and puborectalis and anal sphincter muscles [with different relevant structures shown (64); B], using information from anatomical scans and diffusion tensor imaging (DTI) tractography. A three-dimensional surface model of the muscle, created from a T1-weighted anatomical scan (1 transverse slice is depicted), is shown as a transparent overlay in A. Fiber tracts, which were generated from DTI data coregistered with the anatomical image, were fitted with polynomial curves and extrapolated to ensure that fascicles attach to tendinous structures [see Bolsterlee et al. (9) for more details about these procedures]. In B, color coding of the fiber tracts follows DTI convention and indicates direction of the tract. AP, anterior-posterior; EAS, external anal sphincter; RL, right-left; SI, superior-inferior; trans-perinei, transversus perinei. [B borrowed with permission from Mittal et al. (64).]

tracked in the lower leg (Fig. 4A) and in the human female pelvis (Fig. 4B)].

Critical evaluation. The major strength of DTI is that it provides *in vivo* fiber orientation measurements at high resolution, in whole human muscles and in 3-D. This information is difficult or impossible to obtain with other imaging methods such as ultrasonography, which is primarily 2-D and provides images that are smaller than most human muscles, or conventional MRI scans, which lack the resolution to discern individual muscle fibers. On clinical 3-T MR scanners, DTI scans of whole human limb muscles take ~8–15 min to obtain (depending on resolution, details of the protocol, and scan volume), which makes DTI feasible for both basic physiological studies as well as clinical research on human muscles *in vivo*. These scan times limit the application of DTI to measurements of static muscle structure. Static DTI measurements, however, have also proven useful in investigations of anisotropic dynamic muscle behavior by combining measurements of muscle deformation patterns from dynamic MRI with fiber orientation measurements in a reference (undeformed) state from DTI (28, 38). A challenge in this approach is proper alignment of images obtained with DTI and dynamic sequences.

Although there is strong indirect evidence DTI can provide valid measurements of muscle architecture, quantitative validity has not yet been established in human muscles. DTI measures of muscle architecture have acceptable repeatability (40, 79), and DTI-based reconstructions of muscles exhibit remarkable similarity to the structure of dissected muscles (e.g., 10, 33). Furthermore, DTI-based measurements of muscle architecture of the human gastrocnemius are similar, on average (though not in individual measurements), to measurements made with ultrasound (11). Other data show realistic fascicle lengthening in the gastrocnemius and the soleus muscles when DTI scans are obtained at different muscle-tendon lengths (9, 10).

A challenge for accurate measurements of muscle architecture using DTI tractography is that fiber tracts (the curves that

are obtained through DTI tractography) often terminate intramuscularly or cross over to adjacent muscles. There is evidence that (real) muscle fibers can terminate intramuscularly (72). However, it is unlikely that intramuscular end points of fiber tracts accurately reflect these intramuscular end points of muscle fibers because the location of fiber tract end points depends strongly on the stopping criteria used in DTI tractography and the noise level of the scan. Intramuscular end points of fiber tracts are thus more likely an artifact of DTI tractography, which can be remedied by the application of anatomical constraints that ensure that fiber tracts originate and insert on tendinous structures (9). More thorough validation of DTI-based measurements, especially when made on human muscles using the same scanners and protocols as used for *in vivo* studies, will likely increase the application of DTI in muscle mechanics research.

A potential limitation of DTI in clinical studies is the effect of intramuscular fat on diffusion properties of muscle tissue. The presence of fat leads to higher uncertainty in fiber orientation measurements (22, 89) and may limit the accuracy of DTI-based reconstructions of fiber architecture of diseased muscles, in which fatty infiltration can be significant. It is likely that with improved fat suppression techniques (17) and by filtering the DTI data (60) and excluding regions with high fat content from the analysis (44), the confounding effects of fatty infiltration can be alleviated.

Applications. DTI measurements of fiber orientations have been used to identify differences in mechanical properties (38, 74) and deformation patterns (28, 70) in directions parallel and perpendicular to fibers. On the whole muscle level, DTI has been used in combination with tractography algorithms to measure changes in muscle architecture with passive length changes (9, 10, 62, 83). DTI has also proven useful in biomechanical modeling studies, where information about fiber orientation is essential to accurately simulate the anisotropic behavior of muscle tissue (1, 12, 86). DTI has also been used to study changes in muscle fiber structure (DTI indexes) and

architecture associated with aging (80). In both the lateral and medial gastrocnemius, fiber lengths were shown to be significantly reduced, whereas the primary, secondary, and tertiary diffusion tensor eigenvalues increased with age, underlining the complex dependence of these parameters on fiber atrophy and increased fibrosis.

Only two studies have used DTI to identify differences in muscle properties between healthy and diseased muscles in humans *in vivo* (44, 94). Both these studies focused on differences in diffusion properties and not on differences in muscle architecture. Patients with Duchenne muscular dystrophy were found to have different diffusion properties of some calf muscles compared with a control group (44). It is largely unknown how diffusion properties relate quantitatively to the muscle's microstructure and composition, which strongly limits the interpretation of group differences in diffusion properties. This study also highlighted the potential confounding effect of intramuscular fat and signal-to-noise ratio on the measurement of diffusion properties. Whereas Mittal et al. (64) present visualization of the external anal sphincter muscle and their hypothesized crossing in normal women, Zijta et al. (94) applied DTI to study pelvic floor muscles in women with pelvic floor organ prolapse or related symptoms and a control group. They did not identify differences in diffusion properties in pelvic floor muscles. These studies were performed on small numbers of patients, rendering the results only exploratory.

SUMMARY AND CONCLUSIONS

From this brief review, it is clear that modern medical imaging can provide a wealth of diverse information about muscle mechanics, ranging from muscle architecture through kinematics to intrinsic mechanical properties, both in health and disease. Although MRE and ultrasound SWE can provide maps of muscle mechanical properties, each has its strengths and weaknesses. MRE can provide 3-D maps of muscle elastic and viscous properties, including anisotropic properties, when combined with diffusion imaging. It is also showing promise for measuring nonlinear mechanical properties. However, MRE is expensive, is currently a research technique, and is therefore somewhat difficult to access; data analysis methods vary considerably between researchers, and each data set takes minutes to acquire, limiting its use for studying anything but quasi-static processes. Ultrasound SWE provides 2-D maps of muscle properties and acquires data much more quickly than MRE, although not yet fast enough for dynamic studies. It was also used to analyze the nonlinear behavior of muscle in passive and active conditions (46) and is more widely available because of commercialization of the technique by several ultrasound vendors. However, it is limited to 2-D maps, does not provide viscous parameters, is somewhat limited in its ability to quantify muscle anisotropy, and is more operator dependent. Diffusion imaging provides detailed information on muscle architecture, and the acquisition methods are fairly readily available on clinical 3-T MRI systems; however, it shares the cost and temporal resolution limitations of MRE. These static techniques are complemented by dynamic MRI, which enables measurements of dynamic muscle motion and kinematics, and several techniques are available. Diffusion imaging is also somewhat expensive and more difficult to

access, as some imaging sequences are specialized, and analysis is labor-intensive. Future development to improve the temporal resolution of these imaging methods will expand the range of physiological questions they can be used to study. However, the combination of these methods has already provided major new insights into muscle function, and each has demonstrated potential for use in better understanding changes in muscle passive properties in a broad range of disorders that affect skeletal muscle.

GRANTS

L. E. Bilston is supported by a National Health and Medical Research Council senior research fellowship. A. Nordez is supported by a fellowship from the Auckland University of Technology and grants from Région des Pays de la Loire [Quantification of the Elasticity of Biological Tissues (QUETE) Project, Grant 2015-09035] and the International Society of Biomechanics (Mobility grant). S. Sinha is supported by National Institute of Arthritis and Musculoskeletal and Skin Diseases Grant 5R01-AR-053343-08 and University of California, San Diego, Academic Senate Grant RAD-127B.

DISCLOSURES

No conflicts of interest, financial or otherwise, are declared by the authors.

AUTHOR CONTRIBUTIONS

L.E.B., B.B., A.N., and S.S. conceived and designed this review; L.E.B., B.B., A.N., and S.S. interpreted results of previous research and reported it here; L.E.B., B.B., A.N., and S.S. prepared figures; L.E.B., B.B., A.N., and S.S. drafted manuscript; L.E.B., B.B., A.N., and S.S. edited and revised manuscript; L.E.B., B.B., A.N., and S.S. approved final version of manuscript.

REFERENCES

1. Alipour M, Mithraratne K, Fernandez J. A diffusion-weighted imaging informed continuum model of the rabbit triceps surae complex. *Biomech Model Mechanobiol* 16: 1729–1741, 2017. doi:10.1007/s10237-017-0916-4.
2. Asakawa DS, Blemker SS, Gold GE, Delp SL. In vivo motion of the rectus femoris muscle after tendon transfer surgery. *J Biomech* 35: 1029–1037, 2002. doi:10.1016/S0021-9290(02)00048-9.
3. Asakawa DS, Pappas GP, Blemker SS, Drace JE, Delp SL. Cine phase-contrast magnetic resonance imaging as a tool for quantification of skeletal muscle motion. *Semin Musculoskeletal Radiol* 7: 287–296, 2003. doi:10.1055/s-2004-815676.
4. Basford JR, Jenkyn TR, An KN, Ehman RL, Heers G, Kaufman KR. Evaluation of healthy and diseased muscle with magnetic resonance elastography. *Arch Phys Med Rehabil* 83: 1530–1536, 2002. doi:10.1053/apmr.2002.35472.
5. Bensamoun SF, Ringleb SI, Chen Q, Ehman RL, An KN, Brennan M. Thigh muscle stiffness assessed with magnetic resonance elastography in hyperthyroid patients before and after medical treatment. *J Magn Reson Imaging* 26: 708–713, 2007. doi:10.1002/jmri.21073.
6. Bensamoun SF, Ringleb SI, Littrell L, Chen Q, Brennan M, Ehman RL, An KN. Determination of thigh muscle stiffness using magnetic resonance elastography. *J Magn Reson Imaging* 23: 242–247, 2006. doi:10.1002/jmri.20487.
7. Bercoff J, Tanter M, Fink M. Supersonic shear imaging: a new technique for soft tissue elasticity mapping. *IEEE Trans Ultrason Ferroelectr Freq Control* 51: 396–409, 2004. doi:10.1109/TUFFC.2004.1295425.
8. Bilston LE, Tan K. Measurement of passive skeletal muscle mechanical properties *in vivo*: recent progress, clinical applications, and remaining challenges. *Ann Biomed Eng* 43: 261–273, 2015. doi:10.1007/s10439-014-1186-2.
9. Bolsterlee B, D'Souza A, Gandevia SC, Herbert RD. How does passive lengthening change the architecture of the human medial gastrocnemius muscle? *J Appl Physiol* (1985) 122: 727–738, 2017. doi:10.1152/japplphysiol.00976.2016.
10. Bolsterlee B, Finni T, D'Souza A, Eguchi J, Clarke EC, Herbert RD. Three-dimensional architecture of the whole human soleus muscle *in vivo*. *PeerJ* 6: e4610, 2018. doi:10.7717/peerj.4610.

11. **Bolsterlee B, Veeger HE, van der Helm FCT, Gandevia SC, Herbert RD.** Comparison of measurements of medial gastrocnemius architectural parameters from ultrasound and diffusion tensor images. *J Biomech* 48: 1133–1140, 2015. doi:10.1016/j.jbiomech.2015.01.012.
12. **Brandão S, Parente M, Silva E, Da Roza T, Mascarenhas T, Leitão J, Cunha J, Natal Jorge R, Nunes RG.** Pubovisceralis muscle fiber architecture determination: comparison between biomechanical modeling and diffusion tensor imaging. *Ann Biomed Eng* 45: 1255–1265, 2017. doi:10.1007/s10439-016-1788-y.
13. **Brauck K, Galbán CJ, Maderwald S, Herrmann BL, Ladd ME.** Changes in calf muscle elasticity in hypogonadal males before and after testosterone substitution as monitored by magnetic resonance elastography. *Eur J Endocrinol* 156: 673–678, 2007. doi:10.1530/EJE-06-0694.
14. **Brodie TG.** The extensibility of muscle. *J Anat Physiol* 29: 367, 1895.
15. **Brown EC, Cheng S, McKenzie DK, Butler JE, Gandevia SC, Bilston LE.** Tongue stiffness is lower in patients with obstructive sleep apnea during wakefulness compared with matched control subjects. *Sleep (Basel)* 38: 537–544, 2015. doi:10.5665/sleep.4566.
16. **Brum J, Bernal M, Gennisson JL, Tanter M.** In vivo evaluation of the elastic anisotropy of the human Achilles tendon using shear wave dispersion analysis. *Phys Med Biol* 59: 505–523, 2014. doi:10.1088/0031-9155/59/3/505.
17. **Burakiewicz J, Hooijmans MT, Webb AG, Verschuuren JJ, Niks EH, Kan HE.** Improved olefinic fat suppression in skeletal muscle DTI using a magnitude-based Dixon method. *Magn Reson Med* 79: 152–159, 2018. doi:10.1002/mrm.26655.
18. **Chakouch MK, Charleux F, Bensamoun SF.** Quantifying the elastic property of nine thigh muscles using magnetic resonance elastography. *PLoS One* 10: e0138873, 2015. [Erratum in *PLoS One* 10: e0142958, 2015.] doi:10.1371/journal.pone.0138873.
19. **Chakouch MK, Pouletaut P, Charleux F, Bensamoun SF.** Viscoelastic shear properties of in vivo thigh muscles measured by MR elastography. *J Magn Reson Imaging* 43: 1423–1433, 2016. doi:10.1002/jmri.25105.
20. **Cheng S, Gandevia SC, Green M, Sinkus R, Bilston LE.** Viscoelastic properties of the tongue and soft palate using MR elastography. *J Biomech* 44: 450–454, 2011. doi:10.1016/j.jbiomech.2010.09.027.
21. **Csapo R, Malis V, Hodgson J, Sinha S.** Age-related greater Achilles tendon compliance is not associated with larger plantar flexor muscle fascicle strains in senior women. *J Appl Physiol (1985)* 116: 961–969, 2014. doi:10.1152/jappphysiol.01337.2013.
22. **Damon BM.** Effects of image noise in muscle diffusion tensor (DT)-MRI assessed using numerical simulations. *Magn Reson Med* 60: 934–944, 2008. doi:10.1002/mrm.21707.
23. **Damon BM, Ding Z, Anderson AW, Freyer AS, Gore JC.** Validation of diffusion tensor MRI-based muscle fiber tracking. *Magn Reson Med* 48: 97–104, 2002. doi:10.1002/mrm.10198.
24. **Damon BM, Froeling M, Buck AK, Oudeman J, Ding Z, Nederveen AJ, Bush EC, Strijkers GJ.** Skeletal muscle diffusion tensor-MRI fiber tracking: rationale, data acquisition and analysis methods, applications and future directions. *NMR Biomed* 30: e3563, 2017. doi:10.1002/nbm.3563.
25. **Debernard L, Robert L, Charleux F, Bensamoun SF.** Analysis of thigh muscle stiffness from childhood to adulthood using magnetic resonance elastography (MRE) technique. *Clin Biomech (Bristol, Avon)* 26: 836–840, 2011. doi:10.1016/j.clinbiomech.2011.04.004.
26. **Eby S, Zhao H, Song P, Vareberg BJ, Kinnick R, Greenleaf JF, An KN, Chen S, Brown AW.** Quantitative evaluation of passive muscle stiffness in chronic stroke. *Am J Phys Med Rehabil* 95: 899–910, 2016. doi:10.1097/PHM.0000000000000516.
27. **Eby SF, Song P, Chen S, Chen Q, Greenleaf JF, An KN.** Validation of shear wave elastography in skeletal muscle. *J Biomech* 46: 2381–2387, 2013. doi:10.1016/j.jbiomech.2013.07.033.
28. **Englund EK, Elder CP, Xu Q, Ding Z, Damon BM.** Combined diffusion and strain tensor MRI reveals a heterogeneous, planar pattern of strain development during isometric muscle contraction. *Am J Physiol Regul Integr Comp Physiol* 300: R1079–R1090, 2011. doi:10.1152/ajpregu.00474.2010.
29. **Eriksson Crommert M, Lacourpaille L, Heales LJ, Tucker K, Hug F.** Massage induces an immediate, albeit short-term, reduction in muscle stiffness. *Scand J Med Sci Sports* 25: e490–e496, 2015. doi:10.1111/sms.12341.
30. **Felton SM, Gaige TA, Benner T, Wang R, Reese TG, Wedeen VJ, Gilbert RJ.** Associating the mesoscale fiber organization of the tongue with local strain rate during swallowing. *J Biomech* 41: 1782–1789, 2008. doi:10.1016/j.jbiomech.2008.01.030.
31. **Felton SM, Gaige TA, Reese TG, Wedeen VJ, Gilbert RJ.** Mechanical basis for lingual deformation during the propulsive phase of swallowing as determined by phase-contrast magnetic resonance imaging. *J Appl Physiol (1985)* 103: 255–265, 2007. doi:10.1152/jappphysiol.01070.2006.
32. **Fiorentino NM, Epstein FH, Blemker SS.** Activation and aponeurosis morphology affect in vivo muscle tissue strains near the myotendinous junction. *J Biomech* 45: 647–652, 2012. doi:10.1016/j.jbiomech.2011.12.015.
33. **Froeling M, Nederveen AJ, Heijtel DF, Lataster A, Bos C, Nicolay K, Maas M, Drost MR, Strijkers GJ.** Diffusion-tensor MRI reveals the complex muscle architecture of the human forearm. *J Magn Reson Imaging* 36: 237–248, 2012. doi:10.1002/jmri.23608.
34. **Fung YC.** *Biomechanics: Mechanical Properties of Living Tissues.* New York: Springer, 1993.
35. **Gennisson JL, Deffieux T, Fink M, Tanter M.** Ultrasound elastography: principles and techniques. *Diagn Interv Imaging* 94: 487–495, 2013. doi:10.1016/j.diii.2013.01.022.
36. **Gennisson JL, Deffieux T, Macé E, Montaldo G, Fink M, Tanter M.** Viscoelastic and anisotropic mechanical properties of in vivo muscle tissue assessed by supersonic shear imaging. *Ultrasound Med Biol* 36: 789–801, 2010. doi:10.1016/j.ultrasmedbio.2010.02.013.
37. **Gennisson JL, Provost J, Deffieux T, Papadacci C, Imbault M, Pernot M, Tanter M.** 4-D ultrafast shear-wave imaging. *IEEE Trans Ultrason Ferroelectr Freq Control* 62: 1059–1065, 2015. doi:10.1109/TUFFC.2014.006936.
38. **Green MA, Geng G, Qin E, Sinkus R, Gandevia SC, Bilston LE.** Measuring anisotropic muscle stiffness properties using elastography. *NMR Biomed* 26: 1387–1394, 2013. doi:10.1002/nbm.2964.
39. **Green MA, Sinkus R, Gandevia SC, Herbert RD, Bilston LE.** Measuring changes in muscle stiffness after eccentric exercise using elastography. *NMR Biomed* 25: 852–858, 2012. doi:10.1002/nbm.1801.
40. **Heemskerk AM, Sinha TK, Wilson KJ, Ding Z, Damon BM.** Repeatability of DTI-based skeletal muscle fiber tracking. *NMR Biomed* 23: 294–303, 2010. doi:10.1002/nbm.1463.
41. **Heers G, Jenkyn T, Dresner MA, Klein MO, Basford JR, Kaufman KR, Ehman RL, An KN.** Measurement of muscle activity with magnetic resonance elastography. *Clin Biomech (Bristol, Avon)* 18: 537–542, 2003. doi:10.1016/S0268-0033(03)00070-6.
42. **Hoang PD, Herbert RD, Todd G, Gorman RB, Gandevia SC.** Passive mechanical properties of human gastrocnemius muscle tendon units, muscle fascicles and tendons in vivo. *J Exp Biol* 210: 4159–4168, 2007. doi:10.1242/jeb.002204.
43. **Hong SH, Hong SJ, Yoon JS, Oh CH, Cha JG, Kim HK, Bolster B Jr.** Magnetic resonance elastography (MRE) for measurement of muscle stiffness of the shoulder: feasibility with a 3 T MRI system. *Acta Radiol* 57: 1099–1106, 2016. doi:10.1177/0284185115571987.
44. **Hooijmans MT, Damon BM, Froeling M, Versluis MJ, Burakiewicz J, Verschuuren JJ, Niks EH, Webb AG, Kan HE.** Evaluation of skeletal muscle DTI in patients with Duchenne muscular dystrophy. *NMR Biomed* 28: 1589–1597, 2015. doi:10.1002/nbm.3427.
45. **Hug F, Lacourpaille L, Maïsetti O, Nordez A.** Slack length of gastrocnemius medialis and Achilles tendon occurs at different ankle angles. *J Biomech* 46: 2534–2538, 2013. doi:10.1016/j.jbiomech.2013.07.015.
46. **Hug F, Tucker K, Gennisson JL, Tanter M, Nordez A.** Elastography for muscle biomechanics: toward the estimation of individual muscle force. *Exerc Sport Sci Rev* 43: 125–133, 2015. doi:10.1249/JES.0000000000000049.
47. **Huijing PA, Yaman A, Ozturk C, Yucesoy CA.** Effects of knee joint angle on global and local strains within human triceps surae muscle: MRI analysis indicating in vivo myofascial force transmission between synergistic muscles. *Surg Radiol Anat* 33: 869–879, 2011. doi:10.1007/s00276-011-0863-1.
48. **Jenkyn TR, Ehman RL, An KN.** Noninvasive muscle tension measurement using the novel technique of magnetic resonance elastography (MRE). *J Biomech* 36: 1917–1921, 2003. doi:10.1016/S0021-9290(03)00005-8.
49. **Jensen ER, Morrow DA, Felmlee JP, Murthy NS, Kaufman KR.** Characterization of three dimensional volumetric strain distribution during passive tension of the human tibialis anterior using cine phase contrast MRI. *J Biomech* 49: 3430–3436, 2016. doi:10.1016/j.jbiomech.2016.09.002.
50. **Kim HK, Lindquist DM, Serai SD, Mariappan YK, Wang LL, Merrow AC, McGee KP, Ehman RL, Laor T.** Magnetic resonance imaging

- of pediatric muscular disorders: recent advances and clinical applications. *Radiol Clin North Am* 51: 721–742, 2013. doi:10.1016/j.rcl.2013.03.002.
51. Kinsey ST, Locke BR, Penke B, Moerland TS. Diffusional anisotropy is induced by subcellular barriers in skeletal muscle. *NMR Biomed* 12: 1–7, 1999. doi:10.1002/(SICI)1099-1492(199902)12:1<1:AID-NBM539>3.0.CO;2-V.
52. Korosoglou G, Lehrke S, Wochele A, Hoerig B, Lossnitzer D, Steen H, Giannitsis E, Osman NF, Katus HA. Strain-encoded CMR for the detection of inducible ischemia during intermediate stress. *JACC Cardiovasc Imaging* 3: 361–371, 2010. doi:10.1016/j.jcmg.2009.11.015.
53. Lacourpaille L, Gross R, Hug F, Guével A, Pérone Y, Magot A, Hogrel JY, Nordez A. Effects of Duchenne muscular dystrophy on muscle stiffness and response to electrically-induced muscle contraction: a 12-month follow-up. *Neuromuscul Disord* 27: 214–220, 2017. doi:10.1016/j.nmd.2017.01.001.
54. Lacourpaille L, Hug F, Bouillard K, Hogrel JY, Nordez A. Supersonic shear imaging provides a reliable measurement of resting muscle shear elastic modulus. *Physiol Meas* 33: N19–N28, 2012. doi:10.1088/0967-3334/33/3/N19.
55. Lacourpaille L, Nordez A, Hug F, Couturier A, Dibie C, Guilhem G. Time-course effect of exercise-induced muscle damage on localized muscle mechanical properties assessed using elastography. *Acta Physiol (Oxf)* 211: 135–146, 2014. doi:10.1111/apha.12272.
56. Lee SS, Spear S, Rymer WZ. Quantifying changes in material properties of stroke-impaired muscle. *Clin Biomech (Bristol, Avon)* 30: 269–275, 2015. doi:10.1016/j.clinbiomech.2015.01.004.
57. Le Sant G, Nordez A, Andrade R, Hug F, Freitas S, Gross R. Stiffness mapping of lower leg muscles during passive dorsiflexion. *J Anat* 230: 639–650, 2017. doi:10.1111/joa.12589.
58. Maïsetti O, Hug F, Bouillard K, Nordez A. Characterization of passive elastic properties of the human medial gastrocnemius muscle belly using supersonic shear imaging. *J Biomech* 45: 978–984, 2012. doi:10.1016/j.jbiomech.2012.01.009.
59. Malis V, Sinha U, Csapo R, Narici M, Sinha S. Relationship of changes in strain rate indices estimated from velocity-encoded MR imaging to loss of muscle force following disuse atrophy. *Magn Reson Med* 79: 912–922, 2018. doi:10.1002/mrm.26759.
60. Manjón JV, Coupé P, Concha L, Buades A, Collins DL, Robles M. Diffusion weighted image denoising using overcomplete local PCA. *PLoS One* 8: e73021, 2013. doi:10.1371/journal.pone.0073021.
61. Mazzoli V, Gottwald LM, Peper ES, Froeling M, Coolen BF, Verdonchot N, Sprengers AM, van Ooij P, Strijkers GJ, Nederveen AJ. Accelerated 4D phase contrast MRI in skeletal muscle contraction. *Magn Reson Med* 80: 1799–1811, 2018. doi:10.1002/mrm.27158.
62. Mazzoli V, Oudeman J, Nicolay K, Maas M, Verdonchot N, Sprengers AM, Nederveen AJ, Froeling M, Strijkers GJ. Assessment of passive muscle elongation using diffusion tensor MRI: correlation between fiber length and diffusion coefficients. *NMR Biomed* 29: 1813–1824, 2016. doi:10.1002/nbm.3661.
63. McCullough MB, Domire ZJ, Reed AM, Amin S, Ytterberg SR, Chen Q, An KN. Evaluation of muscles affected by myositis using magnetic resonance elastography. *Muscle Nerve* 43: 585–590, 2011. doi:10.1002/mus.21923.
64. Mittal RK, Bhargava V, Sheean G, Ledgerwood M, Sinha S. Purse-string morphology of external anal sphincter revealed by novel imaging techniques. *Am J Physiol Gastrointest Liver Physiol* 306: G505–G514, 2014. doi:10.1152/ajpgi.00338.2013.
65. Morales-Artacho AJ, Lacourpaille L, Guilhem G. Effects of warm-up on hamstring muscles stiffness: cycling vs foam rolling. *Scand J Med Sci Sports* 27: 1959–1969, 2017. doi:10.1111/sms.12832.
66. Muraki T, Domire ZJ, McCullough MB, Chen Q, An KN. Measurement of stiffness changes in immobilized muscle using magnetic resonance elastography. *Clin Biomech (Bristol, Avon)* 25: 499–503, 2010. doi:10.1016/j.clinbiomech.2010.02.006.
67. Nakamura M, Ikezoe T, Kobayashi T, Umegaki H, Takeno Y, Nishishita S, Ichihashi N. Acute effects of static stretching on muscle hardness of the medial gastrocnemius muscle belly in humans: an ultrasonic shear-wave elastography study. *Ultrasound Med Biol* 40: 1991–1997, 2014. doi:10.1016/j.ultrasmedbio.2014.03.024.
68. Nelissen JL, de Graaf L, Traa WA, Schreurs TJ, Moerman KM, Nederveen AJ, Sinkus R, Oomens CW, Nicolay K, Strijkers GJ. A MRI-compatible combined mechanical loading and MR elastography setup to study deformation-induced skeletal muscle damage in rats. *PLoS One* 12: e0169864, 2017. doi:10.1371/journal.pone.0169864.
69. Oudeman J, Nederveen AJ, Strijkers GJ, Maas M, Luijten PR, Froeling M. Techniques and applications of skeletal muscle diffusion tensor imaging: a review. *J Magn Reson Imaging* 43: 773–788, 2016. doi:10.1002/jmri.25016.
70. Pamuk U, Karakuzu A, Ozturk C, Acar B, Yucesoy CA. Combined magnetic resonance and diffusion tensor imaging analyses provide a powerful tool for in vivo assessment of deformation along human muscle fibers. *J Mech Behav Biomed Mater* 63: 207–219, 2016. doi:10.1016/j.jmbbm.2016.06.031.
71. Proske U, Morgan DL, Gregory JE. Thixotropy in skeletal muscle and in muscle spindles: a review. *Prog Neurobiol* 41: 705–721, 1993. doi:10.1016/0301-0082(93)90032-N.
72. Purslow PP, Trotter JA. The morphology and mechanical properties of endomysium in series-fibred muscles: variations with muscle length. *J Muscle Res Cell Motil* 15: 299–308, 1994. doi:10.1007/BF00123482.
73. Qin EC, Jugé L, Lambert SA, Paradis V, Sinkus R, Bilston LE. In vivo anisotropic mechanical properties of dystrophic skeletal muscles measured by anisotropic MR elastographic imaging: the mdx mouse model of muscular dystrophy. *Radiology* 273: 726–735, 2014. doi:10.1148/radiol.14132661.
74. Qin EC, Sinkus R, Geng G, Cheng S, Green M, Rae CD, Bilston LE. Combining MR elastography and diffusion tensor imaging for the assessment of anisotropic mechanical properties: a phantom study. *J Magn Reson Imaging* 37: 217–226, 2013. doi:10.1002/jmri.23797.
75. Ringleb SI, Bensamoun SF, Chen Q, Manduca A, An KN, Ehman RL. Applications of magnetic resonance elastography to healthy and pathologic skeletal muscle. *J Magn Reson Imaging* 25: 301–309, 2007. doi:10.1002/jmri.20817.
76. Schenk P, Siebert T, Hiepe P, Güllmar D, Reichenbach JR, Wick C, Blickhan R, Böhl M. Determination of three-dimensional muscle architectures: validation of the DTI-based fiber tractography method by manual digitization. *J Anat* 223: 61–68, 2013. doi:10.1111/joa.12062.
77. Selskog P, Heiberg E, Ebberts T, Wigström L, Karlsson M. Kinematics of the heart: strain-rate imaging from time-resolved three-dimensional phase contrast MRI. *IEEE Trans Med Imaging* 21: 1105–1109, 2002. doi:10.1109/TMI.2002.804431.
78. Shiina T, Nightingale KR, Palmeri ML, Hall TJ, Bamber JC, Barr RG, Castera L, Choi BI, Chou Y-H, Cosgrove D, Dietrich CF, Ding H, Amy D, Farrokh A, Ferraioli G, Filice C, Friedrich-Rust M, Nakashima K, Schafer F, Sporea I, Suzuki S, Wilson S, Kudo M. WFUMB guidelines and recommendations for clinical use of ultrasound elastography: Part 1: basic principles and terminology. *Ultrasound Med Biol* 41: 1126–1147, 2015. doi:10.1016/j.ultrasmedbio.2015.03.009.
79. Sinha S, Sinha U. Reproducibility analysis of diffusion tensor indices and fiber architecture of human calf muscles in vivo at 1.5 Tesla in neutral and plantarflexed ankle positions at rest. *J Magn Reson Imaging* 34: 107–119, 2011. doi:10.1002/jmri.22596.
80. Sinha U, Csapo R, Malis V, Xue Y, Sinha S. Age-related differences in diffusion tensor indices and fiber architecture in the medial and lateral gastrocnemius. *J Magn Reson Imaging* 41: 941–953, 2015. doi:10.1002/jmri.24641.
81. Sinha U, Malis V, Csapo R, Moghadasi A, Kinugasa R, Sinha S. Age-related differences in strain rate tensor of the medial gastrocnemius muscle during passive plantarflexion and active isometric contraction using velocity encoded MR imaging: potential index of lateral force transmission. *Magn Reson Med* 73: 1852–1863, 2015. doi:10.1002/mrm.25312.
82. Sinha U, Malis V, Csapo R, Narici M, Sinha S. Shear strain rate from phase contrast velocity encoded MRI: application to study effects of aging in the medial gastrocnemius muscle. *J Magn Reson Imaging* 48: 1351–1357, 2018. doi:10.1002/jmri.26030.
83. Sinha U, Sinha S, Hodgson JA, Edgerton RV. Human soleus muscle architecture at different ankle joint angles from magnetic resonance diffusion tensor imaging. *J Appl Physiol (1985)* 110: 807–819, 2011. doi:10.1152/jappphysiol.00923.2010.
84. Tan K, Jugé L, Hatt A, Cheng S, Bilston LE. Measurement of large strain properties in calf muscles in vivo using magnetic resonance elastography and spatial modulation of magnetization. *NMR Biomed* 31: e3925, 2018. doi:10.1002/nbm.3925.
85. Uffmann K, Maderwald S, Ajaj W, Galban CG, Mateiescu S, Quick HH, Ladd ME. In vivo elasticity measurements of extremity skeletal muscle with MR elastography. *NMR Biomed* 17: 181–190, 2004. doi:10.1002/nbm.887.

86. **Van Donkelaar CC, Kretzers LJ, Bovendeerd PH, Lataster LM, Nicolay K, Janssen JD, Drost MR.** Diffusion tensor imaging in biomechanical studies of skeletal muscle function. *J Anat* 194: 79–88, 1999. doi:[10.1046/j.1469-7580.1999.19410079.x](https://doi.org/10.1046/j.1469-7580.1999.19410079.x).
87. **Van Loocke M, Lyons CG, Simms CK.** A validated model of passive muscle in compression. *J Biomech* 39: 2999–3009, 2006. doi:[10.1016/j.jbiomech.2005.10.016](https://doi.org/10.1016/j.jbiomech.2005.10.016).
88. **van Turnhout M, Peters G, Stekelenburg A, Oomens C.** Passive transverse mechanical properties as a function of temperature of rat skeletal muscle in vitro. *Biorheology* 42: 193–207, 2005.
89. **Williams SE, Heemskerk AM, Welch EB, Li K, Damon BM, Park JH.** Quantitative effects of inclusion of fat on muscle diffusion tensor MRI measurements. *J Magn Reson Imaging* 38: 1292–1297, 2013. doi:[10.1002/jmri.24045](https://doi.org/10.1002/jmri.24045).
90. **Yaman A, Ozturk C, Huijing PA, Yucesoy CA.** Magnetic resonance imaging assessment of mechanical interactions between human lower leg muscles in vivo. *J Biomech Eng* 135: 91003, 2013. doi:[10.1115/1.4024573](https://doi.org/10.1115/1.4024573).
91. **Zhong J, Liu W, Yu X.** Transmural myocardial strain in mouse: quantification of high-resolution MR tagging using harmonic phase (HARP) analysis. *Magn Reson Med* 61: 1368–1373, 2009. doi:[10.1002/mrm.21942](https://doi.org/10.1002/mrm.21942).
92. **Zhong X, Epstein FH, Spottiswoode BS, Helm PA, Blemker SS.** Imaging two-dimensional displacements and strains in skeletal muscle during joint motion by cine DENSE MR. *J Biomech* 41: 532–540, 2008. doi:[10.1016/j.jbiomech.2007.10.026](https://doi.org/10.1016/j.jbiomech.2007.10.026).
93. **Zijta FM, Froeling M, van der Paardt MP, Lakeman MM, Bipat S, van Swijndregt AD, Strijkers GJ, Nederveen AJ, Stoker J.** Feasibility of diffusion tensor imaging (DTI) with fibre tractography of the normal female pelvic floor. *Eur Radiol* 21: 1243–1249, 2011. doi:[10.1007/s00330-010-2044-8](https://doi.org/10.1007/s00330-010-2044-8).
94. **Zijta FM, Lakeman MM, Froeling M, van der Paardt MP, Borstlap CS, Bipat S, Montauban van Swijndregt AD, Strijkers GJ, Roovers JP, Nederveen AJ, Stoker J.** Evaluation of the female pelvic floor in pelvic organ prolapse using 3.0-Tesla diffusion tensor imaging and fibre tractography. *Eur Radiol* 22: 2806–2813, 2012. doi:[10.1007/s00330-012-2548-5](https://doi.org/10.1007/s00330-012-2548-5).